

# Derivation of Flip Ambiguity Probabilities to Facilitate Robust Sensor Network Localization

# Anushiya A Kannan<sup>1 2</sup>, Barış Fidan<sup>2 3</sup>, Guoqiang Mao<sup>1 2</sup>

<sup>1</sup> School of Electrical and Information Engineering, University of Sydney, Australia

<sup>2</sup> National ICT Australia (NICTA) Limited, Australia

<sup>3</sup> Research School of Information Sciences and Engineering, Australian National University, Australia  
 {Anushiya.Kannan,Baris.Fidan,Guoqiang.Mao}@nicta.com.au

**Abstract**—Erroneous local geometric realizations in some parts of the network due to their sensitivity to certain distance measurement errors is a major problem in wireless sensor network localization. This may in turn affect the localization of either the entire network or a large portion of it. This phenomenon is well-described using the notion of “flip ambiguity” in rigid graph theory. In this paper we analytically derive an expression for the flip ambiguity probabilities of arbitrary neighborhoods in two dimensional sensor networks. This probability can be used to mitigate flip ambiguities in two ways: 1) If an unknown sensor finds the probability of flip ambiguity on its location estimate larger than a predefined threshold, it may choose not to localize itself 2) Every known neighbor can be assigned with a confidence factor to its estimated location, reflecting the probability of flip ambiguity; a sensor with an initially unknown location can then choose only those known neighbors with a confidence factor greater than a predefined threshold. A recent study by co-authors have shown that the performance of sequential and cluster based localization schemes in the literature can be significantly improved by correctly identifying and removing neighborhoods with possible flip ambiguities from the localization process. One motivation of this paper is to enhance the performance of the robustness criterion presented in that study by accurately identifying the flip ambiguity probabilities of arbitrary neighborhoods. The various simulations done in this study show that our analytical calculations of the probability of flip ambiguity matches with the simulated detection of the probability very accurately.

## I. INTRODUCTION

A fundamental problem in distance-based sensor network localization is whether a given sensor network with a set of known distances is uniquely localizable. In a graph theoretical framework, a sensor network can be represented by a graph  $G = (V, E)$  with a vertex set  $V$  and an edge set  $E$ , where each vertex  $i \in V$  is uniquely associated with a sensor node  $s_i$  in the network, and each edge  $(i, j) \in E$  corresponds to a sensor pair  $s_i, s_j$  for which the inter-sensor distance  $d_{ij}$  is known [1]–[5]. The planar location information about the sensors corresponds to a 2-dimensional *representation* of the representative graph, which is a mapping  $\bar{p} : V \rightarrow \mathcal{R}^2$ , assigning a location in  $\mathcal{R}^2$  to each vertex in  $V$ . Given a graph  $G = (V, E)$  and a representation of it, the pair  $(G, \bar{p})$  is called a *framework*.

A particular graph property associated with unique localizability of sensor networks is *global rigidity* [4]–[6]. A

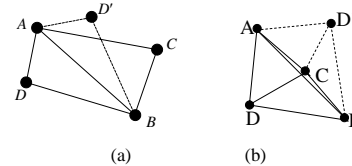


Fig. 1. Flip ambiguity: Reflecting  $D$  through a mirror formed by neighbors, a new realization  $D'$  is obtained without violating the distance constraints. (a) Flip ambiguity in rigid but not globally rigid underlying graph. (b) Flip ambiguity in globally rigid underlying graph with near collinear neighbors.

relaxed form of global rigidity is rigidity. If a framework  $(G, \bar{p})$  is rigid but not globally rigid, there exist two types of discontinuous deformations that can prevent a representation of  $G$  consistent with  $\bar{p}$ , i.e., a representation  $(G, \bar{p}_1)$  satisfying  $\|p(i) - \bar{p}(j)\| = \|\bar{p}_1(i) - \bar{p}_1(j)\|$  for any vertex pair  $i, j \in V$ , which are connected by an edge in  $E$ , from being unique (in the sense that it differs from other such representations at most by translation, rotation or reflection) [3]: flip and discontinuous flex ambiguities. In this paper we focus on flip ambiguities. In flip ambiguities in  $\mathcal{R}^2$ , at least a vertex (sensor node)  $v$  has its all neighbors collinear, which leads to the possibility of neighbors forming a mirror through which  $v$  can be reflected. Fig. 1(a) depicts an example of flip ambiguity.

In real-life sensor networks, the measured distances are erroneous and flip ambiguity may occur even in a network with globally rigid underlying graph [6] with near collinear neighbors (Fig. 1(b)) depending on the sensitivity of those near collinear neighborhoods to such measurement errors.

At the first few iterations of an incremental localization algorithm [7]–[9], only known neighboring nodes for an unknown sensor are the anchor nodes (sensors with known global location information). Availability of these anchor nodes in large numbers are severely limited by the associated costs. Thus the probability of the occurrence of flip ambiguity at the initial iterations is very high. The number of neighbors with initially known location or known estimated location will generally increase with the number of iterations as more and more sensors are localized at each iteration. However, occurrences of flip ambiguities affect not only the location estimate of the associated nodes, but will degrade the location estimates of other nodes in the subsequent iterations, whose known neighborhood include one or more of those nodes with flip ambiguities in their location estimates. This impact can propagate in an avalanche fashion for several iterations degrading location estimates of more and more nodes, as

<sup>2</sup>NICTA is funded by the Australian Government as represented by the Department of Broadband, Communications and the Digital Economy and the Australian Research Council through the ICT Centre of Excellence program.

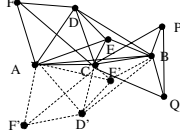


Fig. 2. Initially, locations of  $A, B, C, P$  and  $Q$  are known and  $D, E, F, G, H$  and  $I$  are unknown. At the first iteration,  $D$  and  $E$  uses locations of collinear neighbors  $A, B, C$  and localize itself at  $D'$  and  $E'$  respectively due to flip ambiguity. In the second iteration,  $F$  uses locations of neighbors  $A, C, D$  and localize itself at  $F'$ .

demonstrated in Fig. 2. Similar phenomenon is also seen in cluster localizations [9], [10]. Further details about such phenomenon can be found in [9]. Thus identifying nodes with flip ambiguities at each iteration and removing them from the localization procedure will significantly improve the overall performance of a sensor network localization algorithm.

There exist a number of approaches in the literature to the flip ambiguity problem in different perspectives. The studies [1], [2], [11], [12] have approached this problem by exploring the graph structure. The algorithms in [1], [2] require a dense network in order to maintain global rigidity, to deal with flip ambiguity problem. Global rigidity is only a sufficient condition for unique localization of a sensor network. However, in some cases a priori information may compensate the need of global rigidity [6]. The algorithm in [11] uses the principle of Voronoi diagrams and Delaunay graphs to localize the sensors at the boundaries in order to mitigate flip ambiguities, which also requires the sensors to be sufficiently dense at the boundaries to maintain the rigidity of the Delaunay graph. When the network is sparse, algorithms in [12], [13] suggest to record all possible estimates of each sensor and eliminate incompatible estimates whenever possible, which, in the worst case, recording all possible estimates could result in an explosion in the state space. The studies [9], [10] have approached this problem by identifying possible flip ambiguities in neighborhoods and take necessary actions to eliminate such flip ambiguities. Both these studies assume that the true location and the possible flipped location are symmetrical with respect to a pair of neighboring nodes. Such assumption causes false alarms in the identification of possible flip ambiguities. In this paper, we remove the assumption of symmetry and define an analytical equation for the probability of flip ambiguity of a given neighborhood.

Any prevailing distance based localization algorithm could use these results in two ways: 1) If an unknown sensor finds the probability of flip ambiguity on its location estimate with respect to its known neighborhood to be more than a predefined threshold value, it may choose not to localize itself in that iteration 2) Every known neighbor could be assigned with a confidence factor to its location estimate, reflecting the probability of flip ambiguity; a sensor whose location is to be estimated can then choose only those known neighbors with a confidence factor greater than a predefined threshold during its localization.

## II. PROBLEM FORMULATION

To keep the analysis simple, we consider sensor neighborhoods in the form of fully connected quadruples (FCQs) that

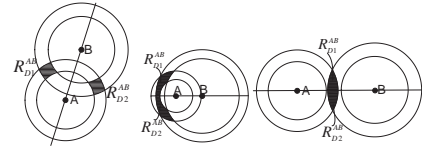


Fig. 3. Location estimate of  $D$  considering two neighbors  $A, B$  and a chosen error bound at a time. Flip occurs with respect to  $AB$  if  $D = (x_D, y_D) \in R_{D_1}^{AB}$  and  $\hat{D} = (\hat{x}, \hat{y}) \in R_{D_2}^{AB}$  or vice versa.

are composed of four sensors which are neighbors of each other, i.e. the distance between any pair is measurable. For any given sensor pair  $(X, Y)$ ,  $d_{XY}$  and  $\bar{d}_{XY}$  are used to denote, respectively, the true distance and measured distance between  $X$  and  $Y$ . Consider an ordered FCQ  $ABCD$  where the locations  $(x_A, y_A)$ ,  $(x_B, y_B)$  and  $(x_C, y_C)$  of sensors  $A, B, C$  and the corresponding measured inter sensor distances  $\bar{d}_{AD}$ ,  $\bar{d}_{BD}$  and  $\bar{d}_{CD}$  from sensor  $D$  to sensors  $A, B$  and  $C$  are known. Assuming the distance measurement error has a known Gaussian distribution with a zero mean and  $\sigma$  standard deviation [14], a threshold  $\bar{\epsilon} > 0$  can be chosen such that the absolute value of the distance measurement error is smaller than the threshold with a certain probability. For example, if  $\bar{\epsilon} = 3\sigma$ , then the probability of the absolute value of the distance measurement error is less than  $\bar{\epsilon}$  is 99%. For a given  $\bar{\epsilon}$ , the relationships between the true distances  $d_{AD}$ ,  $d_{BD}$  and  $d_{CD}$  and the measured distances  $\bar{d}_{AD}$ ,  $\bar{d}_{BD}$  and  $\bar{d}_{CD}$  are,

$$\begin{aligned} d_{AD} &\in [\bar{d}_{AD} - \bar{\epsilon}, \bar{d}_{AD} + \bar{\epsilon}] \\ d_{BD} &\in [\bar{d}_{BD} - \bar{\epsilon}, \bar{d}_{BD} + \bar{\epsilon}] \\ d_{CD} &\in [\bar{d}_{CD} - \bar{\epsilon}, \bar{d}_{CD} + \bar{\epsilon}] \end{aligned} \quad (1)$$

Exploiting (1), we can assert the following constraint on the estimated location  $\hat{D} = (\hat{x}, \hat{y})$  of sensor  $D$ :

$$\begin{aligned} \hat{D} &\in R_D^{ABC} \\ R_D^{ABC} &\triangleq \left\{ (x, y) : \begin{cases} | \| (x, y) - (x_A, y_A) \| - \bar{d}_{AD} | \leq \bar{\epsilon} \text{ and} \\ | \| (x, y) - (x_B, y_B) \| - \bar{d}_{BD} | \leq \bar{\epsilon} \text{ and} \\ | \| (x, y) - (x_C, y_C) \| - \bar{d}_{CD} | \leq \bar{\epsilon} \end{cases} \right\} \end{aligned} \quad (2)$$

Instead, if we only consider constraints imposed by two neighboring sensors  $A$  and  $B$ , without loss of generality, we obtain the relaxed constraint

$$\begin{aligned} \hat{D} &\in R_D^{AB} \\ R_D^{AB} &\triangleq \left\{ (x, y) : \begin{cases} | \| (x, y) - (x_A, y_A) \| - \bar{d}_{AD} | \leq \bar{\epsilon} \text{ and} \\ | \| (x, y) - (x_B, y_B) \| - \bar{d}_{BD} | \leq \bar{\epsilon} \end{cases} \right\} \end{aligned} \quad (3)$$

This region is the intersection of two rings

$$\begin{aligned} | \| (x, y) - (x_A, y_A) \| - \bar{d}_{AD} | &\leq \bar{\epsilon} \text{ and} \\ | \| (x, y) - (x_B, y_B) \| - \bar{d}_{BD} | &\leq \bar{\epsilon} \end{aligned} \quad (4)$$

and is made of two regions  $R_{D_1}^{AB}$  and  $R_{D_2}^{AB}$  as in Fig. 3, i.e.,

$$R_D^{AB} = R_{D_1}^{AB} \cup R_{D_2}^{AB} \quad (5)$$

Fig. 3 also illustrates that if the estimate  $\hat{D}$  is generated based on just  $\bar{d}_{AD}$  and  $\bar{d}_{BD}$ , a flip ambiguity is possible with respect to the line  $AB$ . Also note that, depending on the locations of  $A, B$ , the corresponding measured distances  $\bar{d}_{AD}$ ,  $\bar{d}_{BD}$  and the threshold value  $\bar{\epsilon}$ , the regions  $R_{D_1}^{AB}$  and  $R_{D_2}^{AB}$  may be joint. In such situations, the boundary separating the two regions  $R_{D_1}^{AB}$  and  $R_{D_2}^{AB}$  is taken as the line  $AB$ .

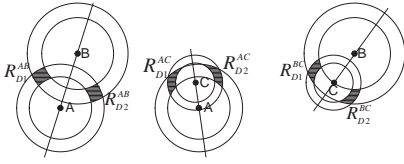


Fig. 4. Possible regions for the location of sensor  $D$  based on considering two neighbors and a chosen error bound at a time.  $R_D^{AB}$  - Possible region for  $D$  given  $A, B, \bar{d}_{AD}, \bar{d}_{BD}, \bar{\epsilon}$ ;  $R_D^{AC}$  - Possible region for  $D$  given  $A, C, \bar{d}_{AD}, \bar{d}_{CD}, \bar{\epsilon}$ ;  $R_D^{BC}$  - Possible region for  $D$  given  $B, C, \bar{d}_{BD}, \bar{d}_{CD}, \bar{\epsilon}$ ;

Similarly, we can consider constraints imposed by neighboring sensor pairs  $(A, C)$  and  $(B, C)$  to define regions  $R_D^{AC}$  and  $R_D^{BC}$  respectively (See Fig. 4) as

$$\begin{aligned} R_D^{AC} &\triangleq \left\{ (x, y) : \begin{cases} \|(x, y) - (x_A, y_A)\| - \bar{d}_{AD} \leq \bar{\epsilon} \text{ and} \\ \|(x, y) - (x_C, y_C)\| - \bar{d}_{CD} \leq \bar{\epsilon} \end{cases} \right\} \\ &= R_{D_1}^{AC} \cup R_{D_2}^{AC} \end{aligned} \quad (6)$$

$$\begin{aligned} R_D^{BC} &\triangleq \left\{ (x, y) : \begin{cases} \|(x, y) - (x_B, y_B)\| - \bar{d}_{BD} \leq \bar{\epsilon} \text{ and} \\ \|(x, y) - (x_C, y_C)\| - \bar{d}_{CD} \leq \bar{\epsilon} \end{cases} \right\} \\ &= R_{D_1}^{BC} \cup R_{D_2}^{BC} \end{aligned} \quad (7)$$

With these definitions, if we consider the constraints imposed by all three neighbors, (2) can be written as

$$\begin{aligned} \hat{D} &\in R_D^{ABC} \\ R_D^{ABC} &= R_D^{AB} \cap R_D^{AC} \cap R_D^{BC} \\ &= (R_{D_1}^{AB} \cup R_{D_2}^{AB}) \cap (R_{D_1}^{AC} \cup R_{D_2}^{AC}) \cap (R_{D_1}^{BC} \cup R_{D_2}^{BC}) \end{aligned} \quad (8)$$

By applying De-Morgan's rule to (8), it follows that  $R_D^{ABC}$  is composed of the following eight disjoint regions:

$$R_{D_{p,q,r}}^{ABC} = R_{D_p}^{AB} \cap R_{D_q}^{AC} \cap R_{D_r}^{BC}; \quad p, q, r \in \{1, 2\} \quad (9)$$

Note that the true location  $D$  has to lie in only one of the eight disjoint regions formulated in (9). Without loss of generality, let us assume that

$$D \in R_{D_{1,1,1}}^{ABC} = R_{D_1}^{AB} \cap R_{D_1}^{AC} \cap R_{D_1}^{BC} \quad (10)$$

Then the eight possible regions given in (9) can be represented by a Venn diagram as in Fig. 5. This Venn diagram consists of three mutually intersecting disks representing the regions  $R_{D_2}^{AB}$ ,  $R_{D_2}^{AC}$ , and  $R_{D_2}^{BC}$ . Note that existence of  $\hat{D}$  in the set represented by any of these three disks corresponds to a flipped realization. For example,  $\hat{D} \in R_{D_2}^{AB}$  implies that there is a flip ambiguity in the location estimate  $\hat{D}$  with respect to the line  $AB$ . Similarly with the help of Fig.5, it is easily seen that the possible location estimates can be grouped into the following four groups.

- **Group 0:**  $\hat{D} \in R_{D_{1,1,1}}^{ABC}$ ;  $(x_D, y_D)$  and  $(\hat{x}, \hat{y})$  are both in  $R_{D_{1,1,1}}^{ABC}$  causing no flip ambiguity.
- **Group 1:**  $\hat{D} \in R_{D_{2,2,2}}^{ABC}$ ;  $(x_D, y_D)$  and  $(\hat{x}, \hat{y})$  are in  $R_{D_{1,1,1}}^{ABC}$  and  $R_{D_{2,2,2}}^{ABC}$  respectively causing possible flip ambiguities with respect to all three lines  $AB, AC$  and  $BC$ .
- **Group 2:**  $\hat{D} \in R_{D_{p,q,r}}^{ABC}$  such that  $p, q, r \in \{1, 2\}$  and  $p+q+r=5$ ;  $(x_D, y_D)$  and  $(\hat{x}, \hat{y})$  are in  $R_{D_{1,1,1}}^{ABC}$  and  $R_{D_{p,q,r}}^{ABC}$  respectively causing possible flip ambiguities with respect to any two lines only:  $AB$  and  $AC$  or  $BC$  and  $AC$  or  $AB$  and  $BC$ .

- **Group 3:**  $\hat{D} \in R_{D_{p,q,r}}^{ABC}$  such that  $p, q, r \in \{1, 2\}$  and  $p+q+r=4$ ;  $(x_D, y_D)$  and  $(\hat{x}, \hat{y})$  are in  $R_{D_{1,1,1}}^{ABC}$  and  $R_{D_{p,q,r}}^{ABC}$  respectively causing possible flip ambiguities with respect to any one line only:  $AB$  or  $AC$  or  $BC$ .

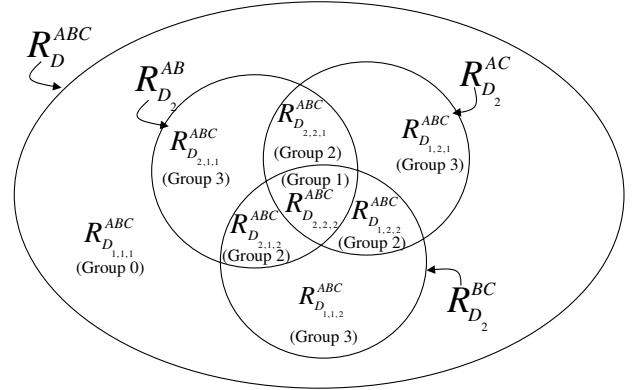


Fig. 5. Venn Diagram representation of (8).

Out of the eight possible regions  $R_{D_{p,q,r}}^{ABC}$  in (9), at-least one of them should be a non-empty region to accommodate the true location of  $D$ . If all but one possible region are null regions, then there is a unique region possible to accommodate the estimated location  $\hat{D}$ , and there would be no possibility for flip realization. But, if two or more regions are non-empty then there is a non-zero probability for the estimated location  $\hat{D}$  to be located inside any of those non-empty regions thereby creating a flip ambiguity problem. Our goal in the next section is to find the probability of having  $\hat{D}$  in each of Group 1, Group 2 and Group 3 flip ambiguity cases.

### III. DERIVATION OF FLIP AMBIGUITY PROBABILITIES

In this section, we derive an analytical equation for the probability of  $\hat{D}$  lying in various regions defined in section II corresponding to flip ambiguity. Firstly, we derive an analytical solution for the case where flip ambiguity occurs only across a single line  $AB$ . We then extend the derivation to all different groups of flip ambiguities mentioned in section II.

Let us first define the probability space  $\Omega$  containing all possible events regarding location estimates  $\hat{D} = (\hat{x}, \hat{y})$ :

$$\Omega = \{(\hat{x}, \hat{y}) \in R_{D_1}^{AB} \cup R_{D_2}^{AB}\} \quad (11)$$

and with the assumption  $D \in R_{D_1}^{AB}$  made in (10), an event set  $\zeta_{AB} \subset \Omega$  containing the location estimation events corresponding to the flipped realization as

$$\zeta_{AB} = \{(\hat{x}, \hat{y}) \in R_{D_2}^{AB}\} \quad (12)$$

Our aim is to find an expression for the probability  $P(\zeta_{AB} | A, B, C, D)$  and then marginalize this probability over all possible locations of  $D$  to find the probability  $P(\zeta_{AB} | A, B, C)$ .

#### A. Calculation of $P(\zeta_{AB} | A, B, C, D)$

Let  $H_C$  denote the open half plane with border line  $AB$  that contains  $C$ , and  $D_{\bar{C}}$  be the complimentary half plane on the other side of  $AB$ . Assuming that  $A, B, C$  are non-collinear,

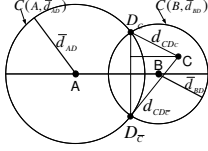


Fig. 6. The effect of  $\bar{d}_{CD}$  in location estimation when circles  $\mathcal{C}(A, \bar{d}_{AD})$  and  $\mathcal{C}(B, \bar{d}_{BD})$  intersect.

$H_C$  and  $H_{\bar{C}}$  are well defined. The two circles  $\mathcal{C}(A, \bar{d}_{AD})$  and  $\mathcal{C}(B, \bar{d}_{BD})$  centered at  $A$  and  $B$  with radius  $\bar{d}_{AD}$  and  $\bar{d}_{BD}$  at two points  $D_C, D_{\bar{C}}$ , one of which is in  $H_C$  and the other in  $H_{\bar{C}}$  as shown in Fig. 6. Without loss of generality, let  $D_C \in H_C$  and  $D_{\bar{C}} \in H_{\bar{C}}$ . When considering only two distance measurements  $\bar{d}_{AD}$  and  $\bar{d}_{BD}$ , both points  $D_C$  and  $D_{\bar{C}}$  will be possible candidates for the location estimate  $\hat{D}$  with  $(d_{A\hat{D}} - \bar{d}_{AD})^2 + (d_{B\hat{D}} - \bar{d}_{BD})^2 = 0$ . When the third distance measurement  $\bar{d}_{CD}$  is included in the localization process, a new candidate for  $\hat{D}$  can be obtained as the minimizer of  $J(\hat{D}) \triangleq (d_{A\hat{D}} - \bar{d}_{AD})^2 + (d_{B\hat{D}} - \bar{d}_{BD})^2 + (d_{C\hat{D}} - \bar{d}_{CD})^2$ . We obtain the following results:

**Proposition 1:** Let  $A, B, C$  be non-collinear. Then  $\hat{D}^* \triangleq \arg \min_{\hat{D}} J(\hat{D})$  satisfies the following:

- i  $\hat{D}^* \in H_C$  when  $0 \leq \bar{d}_{CD} < \lambda_C$
- ii  $\hat{D}^* \in H_{\bar{C}}$  when  $\lambda_C < \bar{d}_{CD} \leq R$

where  $\lambda_C = \frac{d_{CD_C} + d_{CD_{\bar{C}}}}{2}$ .

*Proof:* Noting that  $d_{CD_C} \leq d_{CD_{\bar{C}}}$ , it can be easily seen that  $|d_{CD_C} - \bar{d}_{CD}| < |d_{CD_{\bar{C}}} - \bar{d}_{CD}|$  is always equivalent to  $\bar{d}_{CD} < \lambda_C$ , and  $|d_{CD_C} - \bar{d}_{CD}| > |d_{CD_{\bar{C}}} - \bar{d}_{CD}|$  is always equivalent to  $\bar{d}_{CD} > \lambda_C$ . Hence:

- i When  $0 \leq \bar{d}_{CD} < \lambda_C$ , we have  $|d_{CD_C} - \bar{d}_{CD}| < |d_{CD_{\bar{C}}} - \bar{d}_{CD}|$ . Assume, to obtain contradiction, that  $\hat{D}^* \in H_{\bar{C}}$ . There exists a point  $\hat{D}_2^* \in H_C$  which is symmetric of  $\hat{D}^*$  with respect to  $AB$ . It can be easily seen that  $J(\hat{D}_2^*) < J(\hat{D}^*)$ , which contradicts with the definition of  $\hat{D}^*$ .
- ii When  $\lambda_C < \bar{d}_{CD} \leq R$ , we have  $|d_{CD_C} - \bar{d}_{CD}| > |d_{CD_{\bar{C}}} - \bar{d}_{CD}|$ . Following exactly the same steps as in part (i), we show that  $\hat{D}^*$  cannot be in  $H_C$ . Hence  $\hat{D}^* \in H_{\bar{C}}$ . ■

With the assumption  $D \in R_{D_1}^{AB}$  in (10), a flipped realization occurs when

- i  $\hat{D}^* \in H_C$  and  $R_{D_1}^{AB} \subset H_{\bar{C}}$
- ii  $\hat{D}^* \in H_{\bar{C}}$  and  $R_{D_1}^{AB} \subset H_C$

With this information, we can define two support spaces for events defined in (11) and (12):

$$\Omega' = \{\bar{d}_{AD}, \bar{d}_{BD}, \bar{d}_{CD} \in [0, R] \mid A, B, C, D\} \quad (13)$$

$$\zeta'_{AB} = \begin{cases} \{\bar{d}_{AD}, \bar{d}_{BD} \in [0, R], \bar{d}_{CD} \in [0, \lambda_C] \mid A, B, C, D\} \\ \quad \text{when } R_{D_1}^{AB} \subset H_C \\ \{\bar{d}_{AD}, \bar{d}_{BD} \in [0, R], \bar{d}_{CD} \in [\lambda_C, R] \mid A, B, C, D\} \\ \quad \text{when } R_{D_1}^{AB} \subset H_C \end{cases} \quad (14)$$

Considering the measured distances as the actual distances blurred by Gaussian noise as stated in Section II and assuming

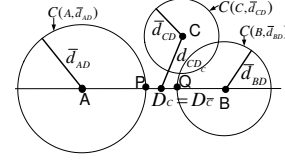


Fig. 7. When circles  $\mathcal{C}(A, \bar{d}_{AD})$  and  $\mathcal{C}(B, \bar{d}_{BD})$  do not intersect,  $D_C \equiv D_{\bar{C}}$ .

that these Gaussian measurement noises are independent of each other, we have the probability distribution functions  $\bar{f}(\bar{d}_{AD}) \triangleq f(\bar{d}_{AD} \mid A, B, C, D)$ ,  $\bar{f}(\bar{d}_{BD}) \triangleq f(\bar{d}_{BD} \mid A, B, C, D)$  and  $\bar{f}(\bar{d}_{CD}) \triangleq f(\bar{d}_{CD} \mid A, B, C, D)$  independent of each other. Therefore defining the binary functions

$$\delta_{CD} = \begin{cases} 1 & \text{If } R_{D_1}^{AB} \subset H_{\bar{C}} \\ 0 & \text{If } R_{D_1}^{AB} \subset H_C \end{cases}$$

$$I_{CD} = \begin{cases} 1 & \text{If } \bar{d}_{CD} \in [0, \min(\lambda_C, R)] \\ 0 & \text{Otherwise} \end{cases}$$

we have

$$\begin{aligned} P(\zeta_{AB} \mid A, B, C, D) &= P(\zeta'_{AB} \mid A, B, C, D) \\ &= \delta_{CD} \int_0^R \int_0^R \int_0^{\min(\lambda_C, R)} \bar{f}(\bar{d}_{CD}) d(\bar{d}_{CD}) \bar{f}(\bar{d}_{BD}) d(\bar{d}_{BD}) \\ &\quad \bar{f}(\bar{d}_{AD}) d(\bar{d}_{AD}) \\ &\quad + (1 - \delta_{CD}) \int_0^R \int_0^R \int_{\min(\lambda_C, R)}^R \bar{f}(\bar{d}_{CD}) d(\bar{d}_{CD}) \\ &\quad \bar{f}(\bar{d}_{BD}) d(\bar{d}_{BD}) \bar{f}(\bar{d}_{AD}) d(\bar{d}_{AD}) \\ &= \int_0^R \int_0^R \int_0^R \left( (\delta_{CD} I_{CD}) + ((1 - \delta_{CD})(1 - I_{CD})) \right) \\ &\quad \bar{f}(\bar{d}_{CD}) d(\bar{d}_{CD}) \bar{f}(\bar{d}_{BD}) d(\bar{d}_{BD}) \bar{f}(\bar{d}_{AD}) d(\bar{d}_{AD}) \quad (15) \end{aligned}$$

Note that the disc transmission model used in the analysis bounds the true inter-sensor distance to be  $\leq R$ , which in turn bounds the measured distances as  $0 \leq \bar{d}_{AD}, \bar{d}_{BD}, \bar{d}_{CD} \leq R + 3\sigma$  with 99% probability. To keep the equations simple, an approximation to these bounds has been made as  $0 \leq \bar{d}_{AD}, \bar{d}_{BD}, \bar{d}_{CD} \leq R$ . Due to this truncation of the measured distances, any calculated probability should be normalized by  $\int_0^R \int_0^R \int_0^R \bar{f}(\bar{d}_{CD}) \bar{f}(\bar{d}_{BD}) \bar{f}(\bar{d}_{AD}) d(\bar{d}_{CD}) d(\bar{d}_{BD}) d(\bar{d}_{AD})$

Also note that, if the circles  $\mathcal{C}(A, \bar{d}_{AD})$  and  $\mathcal{C}(B, \bar{d}_{BD})$  do not intersect as shown in Fig. 7, the points  $D_C$  and  $D_{\bar{C}}$  will coincide with each other and be the mid-point of the line segment  $[PQ]$ . Thus the above analysis holds for both cases,  $\mathcal{C}(A, \bar{d}_{AD})$  and  $\mathcal{C}(B, \bar{d}_{BD})$  intersect and do not intersect.

### B. Calculation of $P(\zeta_{AB} \mid A, B, C)$

In this section, we find the probability  $P(\zeta_{AB} \mid A, B, C)$  by marginalizing the analytical expression obtained in section III-A over all possible locations  $D$  in the planar area  $S$  where  $D$  can be placed. Thus  $P(\zeta_{AB} \mid A, B, C)$  can be written as,

$$P(\zeta_{AB} \mid A, B, C) = \int_S P(\zeta_{AB} \mid A, B, C, D) f(D \mid A, B, C) d(D) \quad (16)$$

Using the fact that the sensors are assumed to have a disc transmission model, for a given neighborhood  $ABC$ , sensor  $D$  could only be placed inside a region  $S$  defined by,

$$S = \left\{ (x_D, y_D) : \begin{cases} \|(x_D, y_D) - (x_A, y_A)\| \leq R^2 \text{ and} \\ \|(x_D, y_D) - (x_B, y_B)\| \leq R^2 \text{ and} \\ \|(x_D, y_D) - (x_C, y_C)\| \leq R^2 \end{cases} \right\}$$

If the sensors are distributed uniformly then,  $f(D | A, B, C) = \frac{1}{A_S}$ , where  $A_S$  is the area of the region  $S$  which can be calculated as described in the Appendix. Defining

$$I_S(D) = \begin{cases} 1 & D \in S \\ 0 & \text{otherwise} \end{cases}$$

we have

$$P(\zeta_{AB} | A, B, C) = \frac{1}{A_S} \int_{\mathcal{R}^2} \int P(\zeta_{AB} | A, B, C, D) I_S(D) d(D) \quad (17)$$

which can be combined with (15) to get

$$P(\zeta_{AB} | A, B, C, D) = \frac{1}{A_S} \int_{\mathcal{R}^2} \int I_S(D) \int_0^R \int_0^R \int_0^R \left( (\delta_{CD} I_{CD}) + ((1 - \delta_{CD})(1 - I_{CD})) \right) \bar{f}(\bar{d}_{CD}) d(\bar{d}_{CD}) \bar{f}(\bar{d}_{BD}) d(\bar{d}_{BD}) \bar{f}(\bar{d}_{AD}) d(\bar{d}_{AD}) d(D) \quad (18)$$

The above processing order of the inter-sensor measurements  $\bar{d}_{AD}$ ,  $\bar{d}_{BD}$ ,  $\bar{d}_{CD}$  has been used without loss of generality, and the analysis below applies to any other order as well with appropriate index modifications. Thus it can be generalized to get  $P(\zeta_{ij} | A, B, C)$  with appropriate index selection of  $i, j, k \in \{A, B, C\}$  and  $i \neq j \neq k$ . If we look at  $\delta_{kD} I_{kD} + (1 - \delta_{kD})(1 - I_{kD})$ , it represents a three dimensional indicator function

$$I_{\zeta_{ij}} = \begin{cases} 1 & \hat{D} \text{ is a flipped realization with respect to line } ij \\ 0 & \text{otherwise} \end{cases}$$

Thus for  $\zeta \in \{\zeta_{ij}, \zeta_{ij} \cap \zeta_{ik}, \zeta_{ij} \cap \zeta_{jk}, \zeta_{ik} \cap \zeta_{jk}, \zeta_{ij} \cap \zeta_{ik} \cap \zeta_{jk}\}$ , (18) can be generalized as

$$P(\zeta | A, B, C) = \frac{1}{A_S} \int_{\mathcal{R}^2} \int I_S \int_0^R \int_0^R \int_0^R I_{\zeta} \bar{f}(\bar{d}_{CD}) d(\bar{d}_{CD}) \bar{f}(\bar{d}_{BD}) d(\bar{d}_{BD}) \bar{f}(\bar{d}_{AD}) d(\bar{d}_{AD}) d(D) \quad (19)$$

where  $I_{\zeta_{ij}} = \delta_{kD} I_{kD} + (1 - \delta_{kD})(1 - I_{kD})$ ,  $I_{\zeta_{ij} \cap \zeta_{ik}} = I_{\zeta_{ij}} I_{\zeta_{ik}}$  and  $I_{\zeta_{ij} \cap \zeta_{ik} \cap \zeta_{jk}} = I_{\zeta_{ij}} I_{\zeta_{ik}} I_{\zeta_{jk}}$  for any permutation of  $i, j, k \in \{A, B, C\}$  and  $i \neq j \neq k$ . With the help of the Venn diagram in Fig. 5, conditional probabilities for Groups 0 – 3 introduced in Section II can be calculated based on the above explanation. For example,  $P(\text{Group 1} | A, B, C) = P(\zeta_{AB} \cap \zeta_{AC} \cap \zeta_{BC} | A, B, C)$

#### IV. NUMERICAL ANALYSIS

We test our analytical solution by comparing the results with various simulation results. In our comparison, fully connected sensor quadruples used are selected from a pool of 4-nodes sensor networks composed of nodes that are uniformly distributed in a region of  $100m \times 100m$  with a transmission range of  $10m$ . The measured distance between the neighbor nodes is blurred by a Gaussian noise [14] as

$$\bar{d}_{ji} = \bar{d}_{ij} + d_{ji} + \mathcal{N}(0, \sigma^2) \quad (20)$$

where the Gaussian noise is truncated such that  $0 \leq \bar{d}_{ji} \leq R$  and  $\sigma$  is varied from  $0.1m$  to  $0.5m$ .

Since the basic building block of all probabilities is  $P(\zeta_{AB} | A, B, C, D)$  and due to space limitations, we are only comparing the results of  $P(\zeta_{AB} | A, B, C, D)$  with respect to arbitrarily placed sensor neighborhoods  $A, B, C$  and  $D$ . Let

the probability  $P(\zeta_{AB} | A, B, C, D)$  obtained via simulations as  $P_S(\zeta_{AB} | A, B, C, D)$  and via our analytical results as  $P_A(\zeta_{AB} | A, B, C, D)$  respectively. Then for  $N_t = 1000$ , we can define  $\Delta_1$  as

$$\Delta_1 = \frac{\sum_{N_t} |P_S(\zeta_{AB} | A, B, C, D) - P_A(\zeta_{AB} | A, B, C, D)|}{N_t} \quad (21)$$

The results shows that the analytical results detects the probability of flip ambiguity accurately.

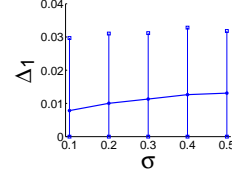


Fig. 8. Comparison of the simulation results  $P_S(\zeta_{AB} | A, B, C, D)$  with our analytical results  $P_A(\zeta_{AB} | A, B, C, D)$  for different  $\sigma$ . Here the vertical lines represent the standard error bar of  $\Delta_1$ .

#### V. PERFORMANCE ENHANCEMENT OF LOCALIZATION ALGORITHMS USING THE FLIP AMBIGUITY PROBABILITY

In this section we use the probability of flip ambiguity calculated using our analytical expression to enhance the performance of the sequential localization algorithm [7], [8], where at each iteration, all unknown nodes with minimum three known neighbors are localized. These known neighbors can be anchors or some nodes defining the local coordinate system. When unknown nodes are localized, they are elevated to anchor status, thereby increasing the chances of unknown nodes being localized in the subsequent iterations.

The localization algorithms in [7], [8] take any FCQ to do trilateration. Instead, we use the probability of flip ambiguity to select the robust FCQ in a particular way as follows: If an unknown node  $i$  with neighborhood  $N_i$  has  $|N_i|$  neighbors, we obtain sets  $\mathcal{C}_3^{|N_i|}$  of all possible FCQs with nodes  $A, B, C \in N_i$  and  $i$ , and find the FCQ with the least probability of flip ambiguity out of all FCQs with a probability of flip ambiguity less than the threshold value of 15%.

In order to evaluate the performance enhancement, 50 different simulated sensor networks with 100 randomly distributed nodes are constructed each with different random seed. Sensor nodes in each of the 50 sensor networks are uniformly distributed in a region of  $100m \times 100m$ . The first 10 sensor nodes are chosen as anchor nodes and are initialized with random coordinates within the boundary. The Gaussian noise in (20) is chosen to have  $\sigma = 0.2m$  and locations of unknown nodes are estimated by minimizing the cost function  $J(\hat{D})$ .

The number of nodes are kept fixed and the transmission range is adjusted in the simulations such that the average node degree varies between 4–25. The average mean squared error in location estimates is calculated and normalized to the transmission range  $R$  as:

$$MSE = \frac{1}{|\{n | V_n \neq \emptyset\}|} \sum_{\substack{n=1 \\ |V_n| \neq 0}}^{50} \frac{1}{|V_n|} \frac{\sum_{i \in V_n} (x_i - \hat{x}_i)^2 + (y_i - \hat{y}_i)^2}{R^2}$$

where  $(\hat{x}_i, \hat{y}_i)$  and  $(x_i, y_i)$  are the estimated and true location of sensor node  $i$ ,  $V_n$  is the set of nodes localized in the  $n^{\text{th}}$  sensor network, and  $|V_n|$  is the number of nodes in  $V_n$ .

To compare different scenarios, FCQs used in trilateration are chosen in four different ways:

- i Any FCQ of  $N_i$ .
- ii Most robust FCQ of  $N_i$  by criterion [9]
- iii Most robust FCQ of  $N_i$  by criterion in [10].
- iv Most robust FCQ of  $N_i$  with probability of flip less than 15%.

From Fig. 9 it can be seen that the average numbers of localized nodes with neighbor selection method (i) and (iv) are more than (ii) and (iii) while the average estimation error of (i) is much larger than (ii), (iii) and (iv). As expected, selection

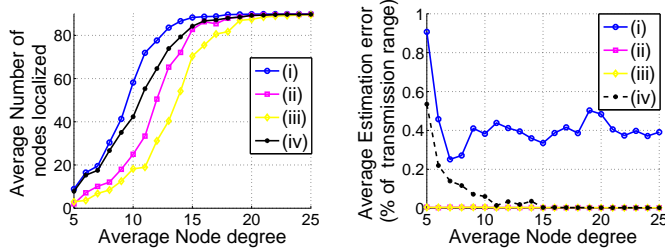


Fig. 9. Performance of different neighbor selection methods (i) to (iv).

method (iv) produced more number of localized nodes with less estimation errors. Due to the threshold value of 15%, some miss-detected flipped realization have caused the average estimation errors to be slightly higher than (ii) and (iii).

Since the reliability of the location estimates is an absolute requirement of any localization algorithm, a robustness criterion for the neighborhood selection to remove those flip ambiguities is essential. For a robustness criterion to be effective, it needs to detect as much flip ambiguities as possible while making as little number of false alarms as possible. From these aspects, the above simulation results show that by choosing a suitable threshold value for (19), the performance can be optimized.

## VI. CONCLUSION AND FUTURE WORK

A recent work of co-authors have well demonstrated that identifying the likelihood of flip ambiguities in location estimates and taking proper action will enhance the performance of localization algorithms significantly.

In this paper we have developed an analytical expression to calculate the probability of flip ambiguity for arbitrary neighborhoods  $ABC$ . This probability can be used either to eliminate neighborhoods which are likely to cause flip ambiguity from the localization process or to decide on confidence factors for the location estimates reflecting the likelihood of flip ambiguities associated with it in order to improve localization performance. Accuracy of our analytical expression as well as the performance enhancement via using this expression in robust localization algorithm based on elimination of flip ambiguities are well demonstrated via simulations.

As a future work, localization algorithms in the literature can be incorporated with confidence factors reflecting the likelihood of flip ambiguities associated with each location

estimate that has been accurately calculated using our analytical results, to enhance their performance.

## REFERENCES

- [1] T. Eren, D. Goldenberg, W. Whiteley, Y. Yang, A. Morse, B. Anderson, and P. Belhumeur, "Rigidity, computation, and randomization in network localisation," in *IEEE INFOCOM*, vol. 4, 2004, pp. 2673 – 2684.
- [2] D. Goldenberg, A. Krishnamurthy, W. Maness, Y. Yang, and A. Young, "Network localization in partially localizable networks," in *IEEE INFOCOM*, 2005, pp. 313 – 326.
- [3] B. Hendrickson, "Conditions for unique graph realizations," *SIAM J. Comput.*, vol. 21, no. 1, pp. 65 – 84, 1992.
- [4] J. Aspnes, T. Eren, D. Goldenberg, A. Morse, W. Whiteley, Y. Yang, B. Anderson, and P. Belhumeur, "A theory of network localization," *IEEE Trans. on Mob. Comp.*, vol. 5, no. 12, pp. 1663 – 1678, 2006.
- [5] B. Anderson, P. Belhumeur, T. Eren, D. Goldenberg, A. Morse, W. Whiteley, and R. Yang, "Graphical properties of easily localizable sensor networks," *Wireless Networks (Springer) Online First*, D.O.I 10.1007/s11276-007-0034-9, 2007.
- [6] G. Mao, B. Fidan, and B. Anderson, "Wireless sensor network localization techniques," *Computer Networks*, vol. 51, no. 10, pp. 2529 – 2553, 2007.
- [7] D. Niculescu and B. Nath, "Dv based positioning in ad hoc networks," *Telecommunication Systems*, vol. 22, no. 1-4, pp. 267 – 280, 2003.
- [8] A. Savvides, C.-C. Han, and M. B. Srivastava, "Dynamic fine-grained localization in ad-hoc networks of sensors," in *ACM SigMobile*, 2001, pp. 166 – 179.
- [9] A. Kannan, B. Fidan, and G. Mao, "Robust distributed sensor network localization based on analysis of flip ambiguities," in *IEEE GlobeCom*, 2008.
- [10] D. Moore, J. Leonard, D. Rus, and S. Teller, "Robust distributed network localization with noisy range measurements," in *2nd ACM Conf. on Embedded Networked Sensor Systems*, 2004, pp. 50 – 61.
- [11] S. Lederer, Y. Wang, and J. Gao, "Connectivity-based localization of large scale sensor networks with complex shape," in *IEEE INFOCOM*, 2008, pp. 789 – 797.
- [12] J. Fang, M. Cao, A. Morse, and B. Anderson, "Localization of sensor networks using sweeps," in *IEEE Conference on Decision and Control*, 2006, pp. 4645 – 4650.
- [13] D. Goldenberg, P. Bihler, M. Cao, J. Fang, B. Anderson, A. Morse, and Y. Yang, "Localization in sparse networks using sweeps," in *ACM/IEEE MobiCom*, 2006, pp. 110 – 121.
- [14] N. Patwari, A. Hero III, M. Perkins, S. Neiyer, and R. ODea, "Relative location estimation in wireless sensor networks," *IEEE Transactions on Signal Processing*, vol. 51, no. 8, pp. 2137 – 2148, 2003.

## APPENDIX

Calculation of  $A_S$ : The area  $A_S$  can be calculated by dividing  $S$  into triangle and/or circular segments. For a

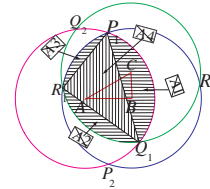


Fig. A.1. The area  $A_S$  where  $D$  can be placed for a given  $A$ ,  $B$  and  $C$ .

given neighborhood in Fig. A.1,  $A_S$  can be calculated as  $A_S = A_1 + A_2 + A_3 + A_4$  where  $A_1$ =area of circular segment  $P_1Q_1 = R^2 \sin^{-1} \frac{d_{P_1Q_1}}{2R} - \frac{R^2}{2} \sin(2 \sin^{-1} \frac{d_{P_1Q_1}}{2R})$ ,  $A_2$ =area of circular segment  $Q_1R_1 = R^2 \sin^{-1} \frac{d_{Q_1R_1}}{2R} - \frac{R^2}{2} \sin(2 \sin^{-1} \frac{d_{Q_1R_1}}{2R})$ ,  $A_3$ =area of circular segment  $P_1R_1 = R^2 \sin^{-1} \frac{d_{P_1R_1}}{2R} - \frac{R^2}{2} \sin(2 \sin^{-1} \frac{d_{P_1R_1}}{2R})$  and  $A_4$ =area of  $\triangle P_1Q_1R_1 = \sqrt{s(s - d_{P_1Q_1})(s - d_{Q_1R_1})(s - d_{P_1R_1})}$  where  $s = \frac{d_{P_1Q_1} + d_{Q_1R_1} + d_{P_1R_1}}{2}$